Memorias del Congreso Nacional de Control Automático
ISSN: 2594-2492

Robust attitude control of multi-rotors for aerial manipulation

J. Díaz-Téllez * J.F. Guerrero-Castellanos. *
L. Villalpando-Portillo *

* *Benemérita Universidad Autónoma de Puebla (BUAP), Facultad de Electrónica, Puebla, CO 72450 Mexico (e-mail:juan.diaztel@alumno.buap.mx,fermi.guerrero@correo.buap.mx, leonardo.villalpandopo@alumno.buap.mx).*

Abstract: In this paper, a robust attitude control applied to multi-rotor UAVs used in load transportation tasks is presented. When a load is attached to the UAV, the distance from the origin of the body-fixed coordinate system to the vehicle's center of gravity is different from zero, which induces external torques and disturbances. The objective is the design of an Active Disturbance Rejection Control (ADRC) to stabilize the attitude subject to external disturbance and uncertain, unknown, unpredictable, or unmodeled dynamics. All these quantities are grouped into a single disturbance vector which is estimated online via an extended state observer (ESO). Then, a quaternion-based feedback is used to stabilize the attitude, which takes into account the maximum torque allowed by the actuators. The effectiveness of this control scheme is evaluated by numerical simulation.

Keywords: Robust Attitude Control, Aerial Transport Operation, Active Disturbance Rejection Control (ADRC) and Swing-Free Load Motion.

1. INTRODUCTION

Recent research on Unmanned Aerial Vehicles (UAVs) has presented improvements in the design and implementation of small and cheap aerial robots which are employed in a wide range of applications. The ability to evading obstacles, maneuvering in confined spaces, hover flight, collect data and interact with different robots make multi-rotors able to solve endless problems like search and rescue operation, temporary communication network, aerial mapping, natural disaster monitoring and kit delivery to name a few. One of the main tasks of multi-rotors is the aerial manipulation, that is to say load transport using gripper, load delivery / retrieving mechanisms and cable-suspend load. This due to the capability of carrying more weight than other UAVs due to its rotors. The aerial transport has many potential applications, due to the different type of cargo that UAVs can carry. For example, purchased goods, food, medicines, vaccine and medical samples in disasters areas, into and out of remote or inaccessible regions. In particular, delivery system with UAVs are taking a big boost, it is expected that revolutionise the way in which customers receive purchased goods. Some advantages of using UAVs as delivery system are the reduction of shipping cost, less manual supervision and faster delivery times since they do not depend on the roadwork or traffic jams. The aerial manipulation is a complicated task and a challenge in the design of control algorithms. The cargo lows down the attitude dynamics due to the increased inertia of the vehicle (Nicotra et al., 2014), the swing-motion of the load produces external torques which change the vehicle's center of gravity and alters the flight characteristics which can result in flight instability. Therefore, it is essential that the flying robot has the ability to adapt to changes in the system dynamics and reduce the swing of the load during assigned maneuvers (Palunko et al., 2012). The typical systems UAVs based in aerial manipulation operation are suspended-load, aerial gripper and delivering/retrieving cargo. Some work related to aerial gripper can be found in (Mellinger et al., 2011) and (Korpela et al., 2011), the cable load suspended can be found in (Palunko et al., 2012), (Sreenath et al., 2013) and (Cruz and Fierro, 2014)

In (Lee et al., 2017) a mathematical model it developed taking into account the variations of a center of gravity. The 3-DOF of swing load is modelled like a pendulum, a cascade PD control algorithm is proposed to attitude and position control for the multi-rotor. The scheme control works well to heavy and light loads, however for the change in mass in the load the response is not smooth. More recently in (Castillo Frasquet et al., 2018) a novel quaternion-based with a disturbance observer-based (DOB) was designed for aggressive attitude maneuvers in the presence of high disturbance.The simulations and experiments show an outstanding control performance in presence of suspended payloads.

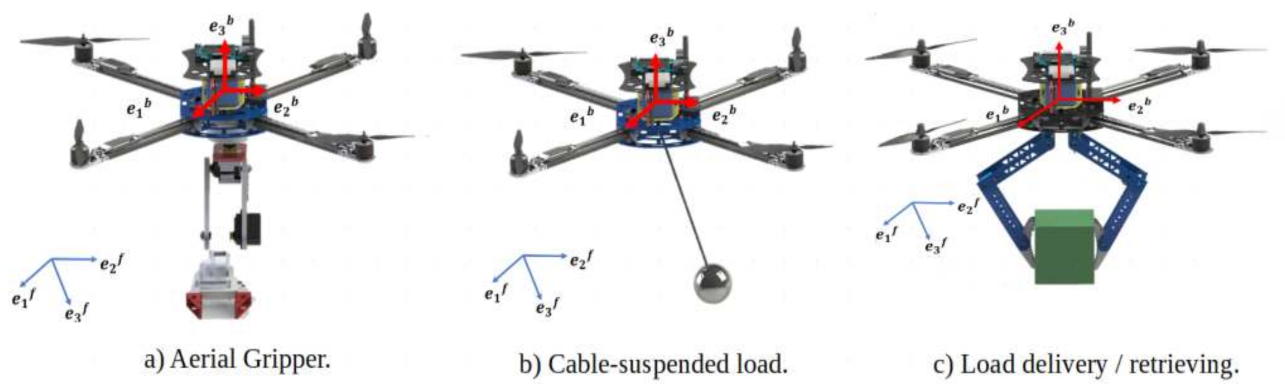

Fig. 1. Load transport mechanisms.

Active Disturbance Rejection Control (ADRC) as originally proposed by J. Han has three components: tracking differentiator, nonlinear feedback control, and nonlinear extended state observer. ADRC is fundamentally based on the possibility of online estimating unknown disturbance inputs affecting the plant behavior by means of suitable observers and proceed to cancelling them via an appropriate feedback control law using the gathered disturbance estimate (Sira-Ramírez et al., 2017). Some works in the field of UAVs using ADRC are (Ma and Jiao, 2017) and (Pulido-Flores et al., 2018). In this paper, we focuses on the robust attitude control of multi-rotors for aerial manipulation via ADRC. We taking into consideration mass and COG variations due to swing load which are modelled like a time-variant endogenous disturbances which is estimate by an extended-state observer (ESO). A bounded controller based on a state feedback controller is proposed using the gathered disturbance estimate. The endogenous disturbance is mitigate and eliminate by the on-line observer. This avoid the interference of the unbalanced load in the autonomous flight. The control law is based on the usage of nested saturation functions to take into account the limitation of actuators.

The rest of the paper is organized as follows. In Section II the mathematical model is presented taking into account the effects of the load and torques induced by external forces. In Section III, the design control and estimation strategies are presented. The attitude tracking is addressed in Section IV. The simulations and experimental result are given in Section V. And finally the concluding remarks and future work are presented in Section VI.

2. SYSTEM MODELING

2.1 Attitude representation

Firstly, assume that a VTOL-UAV can be modeled as a rigid body. Then, consider two orthogonal right-handed coordinate frames: the body coordinate frame, $\mathbf{E}^b = [\boldsymbol{e_1}^b, \boldsymbol{e_2}^b, \boldsymbol{e_3}^b]$, located at the center of mass of the rigid body and the inertial coordinate frame, $\mathbf{E}^f = [\boldsymbol{e_1}^f, \boldsymbol{e_2}^f, \boldsymbol{e_3}^f]$, located at some point in the space (see Fig. 1). The rotation of the body frame $\mathbf{E}^b$ with respect to the fixed frame $\mathbf{E}^f$ is represented by the attitude matrix $R \in SO(3) = \{R \in \mathbb{R}^{3\times3} : R^T R = I, \det R = 1\}$.
The cross product between two vectors ξ, $\chi \; \varepsilon \; \mathbb{R}^{3\times3}$ is represented by a matrix multiplication $[\xi^\times]\chi = \xi \times \chi$, where $[\xi^\times]$ is well know sknew-symmetric matrix.

Hence, a unit quaternion, $q \in \mathbb{S}^3$, is defined as

$$q := \begin{pmatrix} \cos\frac{\beta}{2} \\ e_v \sin\frac{\beta}{2} \end{pmatrix} = \begin{pmatrix} q_0 \\ q_v \end{pmatrix} \in \mathbb{S}^3 \tag{1}$$

$q_v = (q_1 \quad q_2 \quad q_3)^T \in \mathbb{R}^3$ and $q_0 \in \mathbb{R}$ are known as the vector and scalar parts of the quaternion respectively. q represents an element of $SO(3)$ through the map $\mathcal{R} : \mathbb{S}^3 \to SO(3)$ known as Rodrigues formula

$$\mathcal{R} := I_3 + 2q_0[q_v^\times] + 2[q_v^\times]^2 \tag{2}$$

Note that $R = \mathcal{R}(q) = \mathcal{R}(-q)$ for each $q \in \mathbb{S}^3$, *i.e.* quaternions q and $-q$ represent the same physical attitude. The rotation matrix $R \in SO(3)$ serves as a transformation that brings the body frame into the body frame.
The attitude error is used to quantify the mismatch between two attitudes. If q defines the current attitude quaternion and q_d is the desired quaternion, *i.e.* the desired orientation, then the quaternion that represents the attitude error between the current orientation and the desired one is given by

$$\tilde{q} = q_d^{-1} \otimes q = (\tilde{q}_0 \; \tilde{q}_v{}^T)^T \tag{3}$$

where q^{-1} is the complementary rotation of the quaternion q which is given by $q^{-1} = (q_0 \quad -q_v^T)^T$ and $\otimes$ denotes the quaternion multiplication (Shuster, 1993). In the case that the current quaternion and the desired one coincide, the quaternion error becomes $\tilde{q} = (\pm 1 \; 0^T)^T$.

2.2 Motion's equations of the VTOL-UAV

The study of UAV motion has two main concepts: the rotational and translational motion. According to the aforementioned and to (Guerrero-Castellanos et al., 2011), the six degrees of freedom model (position and attitude) of the system can be separated into translational and rotational motions.

2.3 Attitude representation

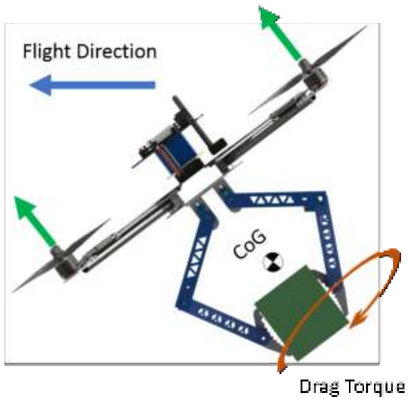

Fig. 2. Load transport mechanisms.

Only the rotational motion is considered, taking into account the effects of that the aerial mechanisms like grippers, load delivery / retrieving and cable-suspend load. When the multirotor flies forward, the induced airflow will derive the drag force on the propeller (see Fig. 2) which will cause a drag torque will make the pitch angle turn zero, besides the wind interference will give to a similar effect but in the opposite direction, then the drag torque will cause the increase in the pitch angle until the multirotor is turned over. Taking into account the above we can modeling the multirotor as:

$$\Sigma_R : \begin{cases} \dot{q} = \dfrac{1}{2}\begin{pmatrix} -q_v^T \\ I_3 q_0 + [q_v^\times] \end{pmatrix}\omega \\ J\dot{\omega} = -[\omega^\times]J\omega + \Gamma + \Gamma_d \\ \quad + \Gamma_g + R_c T \boldsymbol{e_3}^b \end{cases} \tag{4}$$

$\omega \in \mathbb{R}^3$ denotes the angular velocity vector of the body coordinate frame, $\mathbf{E}^b$ relative to the inertial coordinate frame, $\mathbf{E}^f$, expressed in $\mathbf{E}^b$, $\Gamma \in \mathbb{R}^3$ depends on the couples generated by the actuators, and as a consequence, it represents the control signal. Furthermore, several torques and forces acting on the aircraft are being considered. They can be classified in endogenous disturbances (which are dependent upon internal variables) and exogenous disturbance (which are generated by the environment). The former group are gravity force, the gyroscopic torque associated with rotor crafts denoted by Γ_g, the coupling between the trust force and the actuated torque denoted by $R_c T\boldsymbol{e_3}^b$ which arise for the fact that the thrust force vector $T\boldsymbol{e_3}^b$ may not be applied exactly to the vehicle's center of mass. The latter group is the torque induced by all external forces Γ_d, whose value depend on the translational and angular acceleration, and time-variant external disturbance, including wind, which does not depend on the vehicles position and motion.

3. PROBLEM STATEMENT

The main purpose of the present paper is to design control and estimation strategies that would be able to ensure the stabilization of an UAV-VTOL specifically a four-rotor helicopter.

As a result, the system error dynamics are given by

$$\Sigma_{R_e} : \begin{cases} \dot{\tilde{q}} = \dfrac{1}{2}\begin{pmatrix} -\tilde{q}_v^T \\ I_3 \tilde{q}_0 + [\tilde{q}_v^\times] \end{pmatrix}\omega_e \\ J\dot{\omega}_e = -[(\omega_e+\omega_r)^\times]J(\omega_e+\omega_r) + [\omega_e^\times]\omega_r \\ \quad - R^T(\tilde{G})\dot{\omega}_d + \Gamma + \Gamma_d + \Gamma_g + R_c T\boldsymbol{e_3}^b \end{cases} \tag{5}$$

Where $\omega_e = \omega - \omega_r$ with $\omega_r = R^T(\tilde{q})\omega_d$. As a consequence, an Active Disturbance Rejection Control (ADRC) to tracking a desired attitude despite the external disturbance will be first designed. To achieve this objective, an Extended State Observer (ESO) will be designed to estimate on-line the unknown disturbances and cancel them by injecting the output of ESO into the feedback loop. Furthermore, the proposed feedback controls take into account the physical constraints and limitations of the body's structure and actuation. This is ensured by a saturation of the control torque in order to avoid unwanted damage and to maximize the system's actuators effectiveness. This can be formulated as:

$$\Gamma_j \in [-\bar{\Gamma}_j, \bar{\Gamma}_j], \quad j \in \{1,2,3\}$$

where $\bar{\Gamma}_j$ represent the bounds of the control torque.

4. ADRC DESIGN FOR ATTITUDE TRACKING

In this section an attitude trajectory tracking for an UAV-VTOL is addressed. In order to tackle this problem, let us consider first the attitude dynamics error equation

$$\dot{\omega_e} = J^{-1}\left[\Gamma + \xi(\dot{p}, \ddot{p}, R, \omega, \dot{\omega}, d(t))\right] \tag{6}$$

where

$$\begin{aligned} \xi(t) = &-[(\omega_e+\omega_r)^\times]J(\omega_e+\omega_r) + [\omega_e^\times]\omega_r \\ &- R^T(\tilde{q})\dot{\omega}_d + \Gamma_d + \Gamma_G + R_c T\boldsymbol{e_3}^b \end{aligned} \tag{7}$$

i.e. $\xi(\cdot)$ is constituted by the sum of the endogenous perturbation and the exogenous one. Then a control strategy based on the Active Disturbance Rejection Control (ADRC) technique is proposed. The function, $\xi(t)$, will be estimated through of the Extended State Observer (ESO), which is based on the system's dynamic (6).
For this purpose, one has the following assumptions:

- ω and q are measured, such that ω_e is always available;
- The inertia matrix is diagonal, i.e. $J = (J_1, J_2, J_3)$ with $J_1 = J_2 < J_3$ and its nominal value is known;
- The perturbation function $\xi(t)$ is a uniformly absolutely bounded disturbance, i.e. $\sup_t \|\xi(\cdot)\| = \|\xi(t)\|_\infty \le K_0$.
- The angular velocity error estimation, the disturbance estimation and its time derivative will be denoted by $\hat{\omega}_e$, η_1 and η_2, respectively;

4.1 ESO design for the attitude dynamics

Let $e = \omega_e - \hat{\omega}_e$ be the estimation error, through (6), we propose the following extended state observer

$$\Sigma_{ESO} := \begin{cases} \dot{\hat{\omega}}_e = J^{-1}\Gamma + \eta_1 + L_2 e \\ \dot{\eta}_1 = \eta_2 + L_1 e \\ \dot{\eta}_2 = L_0 e \end{cases} \tag{8}$$

where $\hat{\omega}_e$ is the estimated angular velocity error, the $\eta_1 = J^{-1}\hat{\xi}$ and $\eta_2 = J^{-1}\dot{\hat{\xi}}$ are the disturbance estimation and its time derivative respectively. The set of matrices $L_2 = (l_2, l_2, l_2)$, $L_1 = (l_1, l_1, l_1)$, $L_0 = (l_0, l_0, l_0)$ are selected with the assistance of a desired closed-loop Hurwitz polynomial of third-order.

4.2 Active disturbance rejection bounded attitude control

In this subsection, a control law will be designed to maintain a desired attitude from any initial condition. The goal is to bring ω_e and q_v to zero when $t \to \infty$.

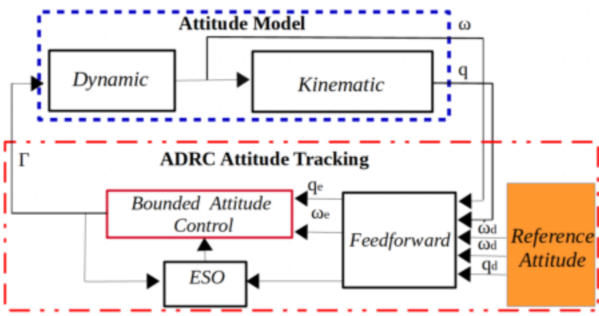

Fig. 3. Structure Scheme Control.

Given a positive constant M, a continuous, nondecreasing function $\sigma_M : \mathbb{R} \to \mathbb{R}$ is defined by

$$\begin{array}{l} (1)\sigma_M = s \text{ if } |s| < M; \\ (2)\sigma_M = \text{sign}(s)M \text{ elsewhere}; \end{array} \tag{9}$$

Let us remember that the disturbance vector ξ is bounded, *i.e.* $\sup_t \ |\xi_{d_i}(\cdot)| \leq K_0$. Furthermore, let K_{0_i} denote the bound for the disturbance function about the i^{th} axis. Assuming that after a sufficient long time ξ is estimated via the observer (8), that is, $\hat{\xi} = J\eta_1$, then one has the following result.

Consider the rigid body rotational dynamics described by (4) with the following bounded control inputs $\Gamma = (\Gamma_1 \ \Gamma_2 \ \Gamma_3)^T$ such that

$$\Gamma_i = -\sigma_{M_{i2}}\left(\hat{\xi}_i + \sigma_{M_{i1}}(\bar{\lambda}_i[\omega_{e_i} + \rho_i \tilde{q}_i])\right) \tag{10}$$

with $i \in \{1, 2, 3\}$ and where $\sigma_{M_{i1}}$ and $\sigma_{M_{i2}}$ are saturation functions such that $K_{0_i} < M_{i2} - M_{i1}$ and $M_{1i} \geq 3\bar{\lambda}_i\rho_i$. $\bar{\lambda}_i$ and ρ_i are positive parameters. $\hat{\xi} = J\eta_1$ with η_1 the estimation of the unknown disturbance $J^{-1}\xi$. Then the inputs (10) stabilize robustly (4) to the origin of the error space $(1 \ 0^T \ 0^T)^T$ (*i.e.* $\tilde{q}_0 = 1, \tilde{q}_v = 0$ and $\omega_e = 0$) with a domain of attraction equal to $\mathbb{S}^3 \times \mathbb{R}^3 \setminus (-1 \ 0^T \ 0^T)^T$.

Due to the reduced space the proof si not given. However, we would like to present the idea behind the construction of feedback (10). The proposed control law is composed of a feedforward term represented by $\hat{\xi}_i$ and the feedback term $\sigma_{M_{i1}}(\cdot)$. Furthermore, both terms represent the argument for the function $\sigma_{M_{i2}}$ which at the same time represents the bound of the control torque Γ_i. The objective is to design a control law which assures that physically, the system has the capability to tracking a desired attitude while it rejects the total disturbance ξ. Since disturbance ξ_i about the i^{th} axis is uniformly bounded by K_{0_i}, the closed-loop stability will be guaranteed if the following constraint is satisfied $K_{0_i} + M_{i1} < M_{i2}$. Actually, M_{i2} plays the role of an Explicit Reference Governor (Garone and Nicotra, 2016) which ensures constraint satisfaction by suitably manipulating the feedforward and the feedback term.

5. SIMULATIONS AND RESULTS

In this sections, the controller proposed were simulated in MatLab according to the Fig: 3. All the simulations are carried out using the following inertial diagonal matrix ($J_{xx} = 1.0947 \times 10^{-5} Kg \ m^2, J_{yy} = 1.1019 \times 10^{-5} Kg \ m^2, J_{zz} = 2.112 \times 10^{-5} Kg \ m^2$). The maximum amplitude torque is given by :

$$\overline{\Gamma} = \begin{pmatrix} \overline{\Gamma}_1 \\ \overline{\Gamma}_2 \\ \overline{\Gamma}_3 \end{pmatrix} = \begin{pmatrix} 9.6 \times 10^{-3} Nm \\ 9.6 \times 10^{-3} Nm \\ 4.6 \times 10^{-3} Nm \end{pmatrix} \tag{11}$$

The endogenous and exogenous disturbance $\xi(\cdot)$ was supplied to the multirotor dynamics system with the following proposed function (12).

$$\xi = \begin{pmatrix} 0.001[1 + \exp(-sin(0.3t)sin(0.3t)))] \cos 0.5t \\ 0.001[1 + \exp(-sin(0.3t)sin(0.3t))] \cos 0.6t \\ 0.001 \cos 0.7t \end{pmatrix} \tag{12}$$

$\xi = (0.004 \quad 0.004 \quad 0.002)^T$, which represent the 40% of the torques generated by the actuator.

The Fig: 4 shown the disturbance and the estimated disturbance. Note that the trajectory is performed simultaneously in the three axis and the response of the ESO follow the trajectory successfully. The observers parameters are $L_2 = (791 \quad 791 \quad 791)^T$, $L_1 = (6026 \quad 6026 \quad 6026)^T$ and $L_0 = (17160 \quad 17160 \quad 17160)^T$. The Fig. 5 shows the zero convergence of the disturbance estimation error. This figure shows the effectiveness of the observer to estimate the disturbances. The attitude tracking control scheme is addressed, once the disturbance is gen-

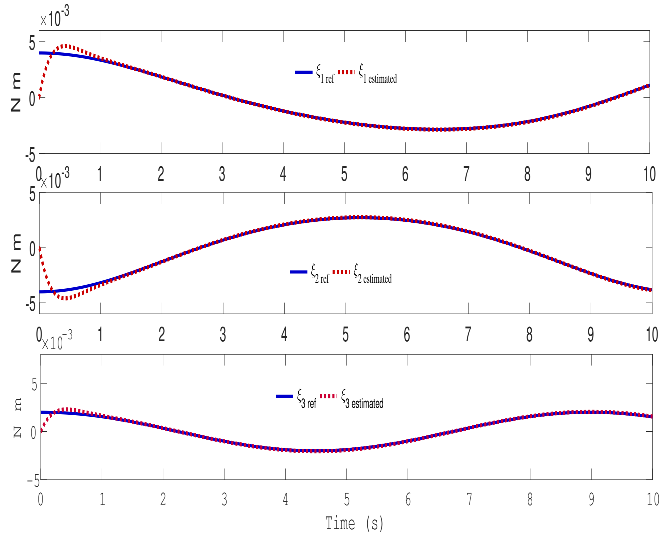

Fig. 4. Evolution of External and Estimated Disturbance $(\xi(\cdot), \hat{\xi}(\cdot)$.

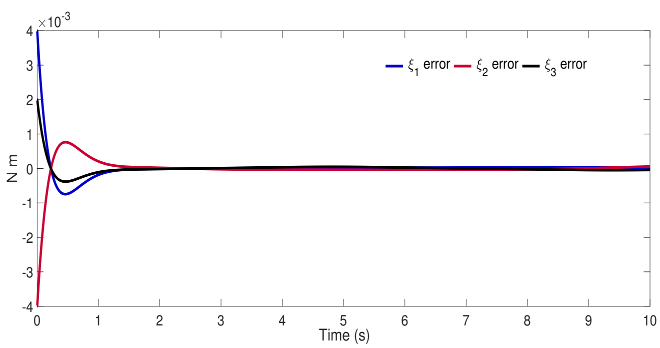

Fig. 5. Disturbance error $\tilde{\xi}$.

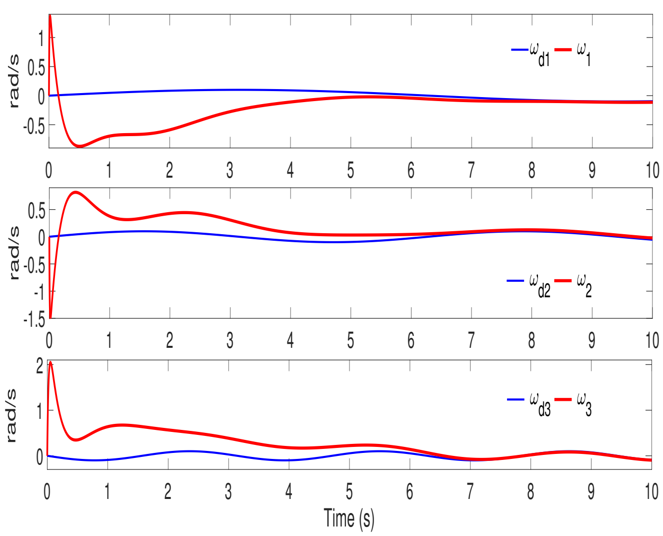

Fig. 6. Evolution of Angular velocity desired ω_d and Angular velocity ω

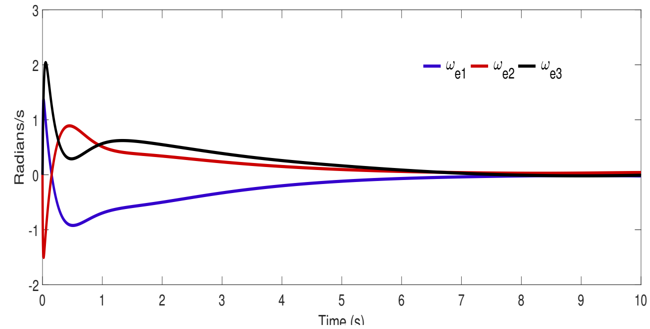

Fig. 7. Angular velocity error ω_e.

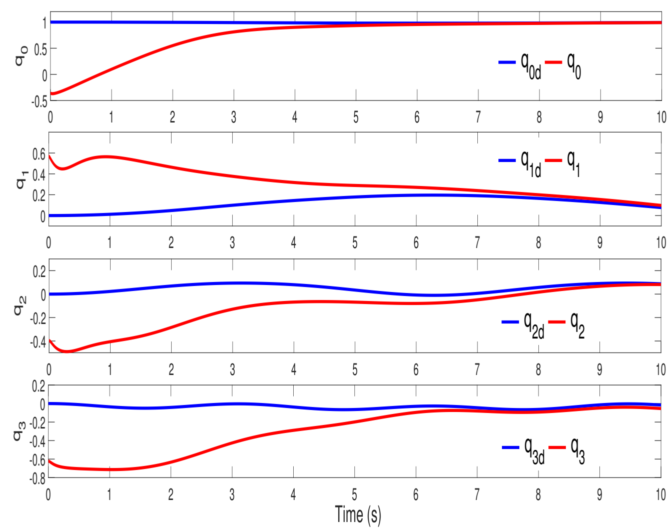

Fig. 8. Evolutions of Attitude desired q_d and Attitude q.

erated by the observer. We proposed a desired variant trajectory in time for the angular velocity $\omega_d = (0.1\sin 0.5t \quad 0.1\sin t \quad 0.1\sin 2t)^T$. In the Fig. 6 shows the angular velocity desired ω_d and the system response ω. The Fig: 7 shown the evolution of the error angular velocity ω_e The responses converges to zero ensuring the stabilization in the tracking problem. The attitude reference desired is shown in the Fig. 8 , this is calculated by a simple derived in the reference attitude block (see Fig. 3).

The Fig. 9 shows the control torque to the attitude tracking stabilization. Note that the response does not exceed the maximum torque allowed in the actuators (11). The Fig: 10 shows the evolution of the attitude error evolution $\tilde{q}$. Note that the responses converges to zero ensuring the stabilization in the tracking problem. We can show the robustness of the control law to compensate and stabilize multi-rotors which are subject to aerial manipulation.

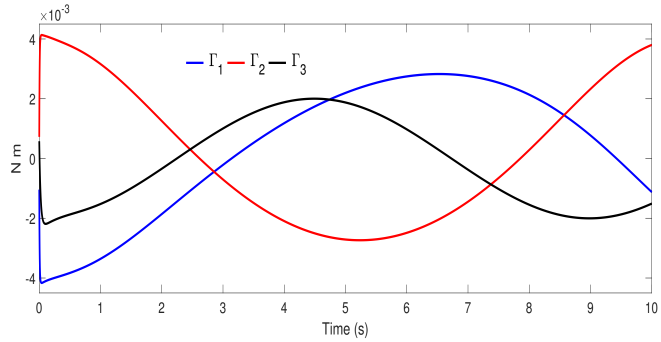

Fig. 9. Control signal based on the ADRC. Γ

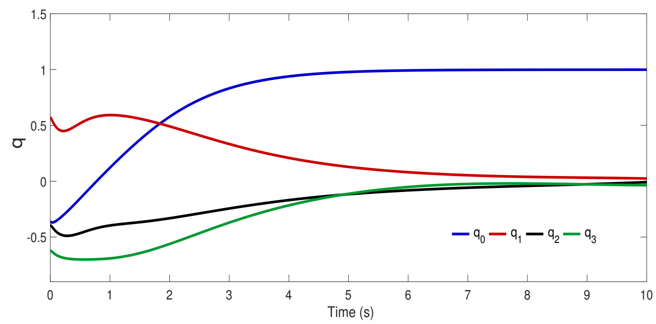

Fig. 10. Attitude error $\tilde{q}$.

6. CONCLUSION

In this paper, a robust attitude control for multi-rotor UAV with aerial manipulation was presented. The simulations performed show that ESO actively estimates the disturbance and its derivative, together with a quaternion-based feedback solve the trajectory tracking problem. The control shows robustness to endogenous and exogenous disturbances, in addition to showing a response free of oscillations, which makes it attractive to solve the problem of aerial manipulation. As future work, the ADRC will be implemented on an embedded system based on the ARM processors. The tests will be carried out through the different mechanisms of aerial manipulation.

REFERENCES

Castillo Frasquet, A., Sanz, R., and García, P. (2018). Disturbance observer-based quadrotor attitude tracking control for aggressive maneuvers. *Control Engineering Practice*, 82, 14–23. doi:10.1016/j.conengprac.2018.09.016.

Cruz, P. and Fierro, R. (2014). Autonomous lift of a cable-suspended load by an unmanned aerial robot. In *2014 IEEE Conference on Control Applications (CCA)*, 802–807. doi:10.1109/CCA.2014.6981439.

Garone, E. and Nicotra, M.M. (2016). Explicit reference governor for constrained nonlinear systems. *IEEE Transactions on Automatic Control*, 61(5), 1379–1384.

Guerrero-Castellanos, J.F., Marchand, N., Hably, A., Lesecq, S., and Delamare, J. (2011). Bounded attitude control of rigid bodies: Real-time experimentation to a quadrotor mini-helicopter. *Control Engineering Practice*, 19(8), 790–797.

Korpela, C.M., Danko, T.W., and Oh, P.Y. (2011). Designing a system for mobile manipulation from an unmanned aerial vehicle. In *2011 IEEE Conference on Technologies for Practical Robot Applications*, 109–114. doi:10.1109/TEPRA.2011.5753491.

Lee, S., Giri, D.K., and Son, H. (2017). Modeling and control of quadrotor uav subject to variations in center of gravity and mass. In *2017 14th International Conference on Ubiquitous Robots and Ambient Intelligence (URAI)*, 85–90. doi:10.1109/URAI.2017.7992893.

Ma, Z. and Jiao, S.M. (2017). Research on the attitude control of quad-rotor uav based on active disturbance rejection control. In *2017 3rd IEEE International Conference on Control Science and Systems Engineering (ICCSSE)*, 45–49. doi:10.1109/CCSSE.2017.8087892.

Mellinger, D., Lindsey, Q., Shomin, M., and Kumar, V. (2011). Design, modeling, estimation and control for aerial grasping and manipulation. In *2011 IEEE/RSJ International Conference on Intelligent Robots and Systems*, 2668–2673. doi:10.1109/IROS.2011.6094871.

Nicotra, M.M., Garone, E., Naldi, R., and Marconi, L. (2014). Nested saturation control of an uav carrying a suspended load. In *2014 American Control Conference*, 3585–3590. doi:10.1109/ACC.2014.6859222.

Palunko, I., Cruz, P., and Fierro, R. (2012). Agile load transportation : Safe and efficient load manipulation with aerial robots. *IEEE Robotics Automation Magazine*, 19(3), 69–79. doi:10.1109/MRA.2012.2205617.

Pulido-Flores, A., Guerrero-Castellanos, J.F., Linares-Flores, J., Maya-Rueda, S.E., Alvarez-Muñoz, J.U., Escareno, J., and Mino-Aguilar, G. (2018). Active disturbance rejection control for attitude stabilization of multi-rotors uavs with bounded inputs. In *2018 International Conference on Unmanned Aircraft Systems (ICUAS)*, 1181–1188. doi:10.1109/ICUAS.2018.8453454.

Shuster, M.D. (1993). A survey of attitude representations. *Navigation*, 8(9), 439–517.

Sira-Ramírez, H., Luviano-Juárez, A., Ramírez-Neria, M., and Zurita-Bustamante, E. (2017). *Active Disturbance Rejection Control of Dynamic Systems: A Flatness Based Approach.*

Sreenath, K., Lee, T., and Kumar, V. (2013). Geometric control and differential flatness of a quadrotor uav with a cable-suspended load. In *52nd IEEE Conference on Decision and Control*, 2269–2274. doi:10.1109/CDC.2013.6760219.

